ELSEVIER

Applied Numerical Mathematics 25 (1997) 193–205

APPLIED NUMERICAL MATHEMATICS

On the stability of implicit–explicit linear multistep methods ☆

J. Frank *, W. Hundsdorfer, J.G. Verwer

CWI, P.O. Box 94079, 1090 GB Amsterdam, The Netherlands

Abstract

In many applications, such as atmospheric chemistry, large systems of ordinary differential equations (ODEs) with both stiff and nonstiff parts have to be solved numerically. A popular approach in such cases is to integrate the stiff parts implicitly and the nonstiff parts explicitly. In this paper we study a class of implicit–explicit (IMEX) linear multistep methods intended for such applications. The paper focuses on the linear stability of popular second order methods like extrapolated BDF, Crank–Nicolson leap-frog and a particular class of Adams methods. We present results for problems with decoupled eigenvalues and comment on some specific CFL restrictions associated with advection terms. © 1997 Elsevier Science B.V.

Keywords: Implicit–explicit methods; Linear multistep methods; Method of lines; Stability

1. Implicit–explicit linear multistep methods

When adopting the method of lines approach, space discretization of multi-space dimensional, time dependent PDE problems results in large systems of ODEs which are to be integrated in time by an appropriate time stepping scheme. Frequently in such applications one is confronted with problems having both stiff and nonstiff parts. Here the term nonstiff is used in a loose way to indicate terms that may be solved efficiently in an explicit way. For example, in atmospheric chemistry one may have a nonstiff horizontal advection term and a stiff term containing chemical reactions and vertical diffusion, see, for instance, Verwer et al. [10], Zlatev [12]. In such cases it is desirable to treat the stiff part with an implicit scheme while applying an explicit scheme to the nonstiff part.

In this paper we look at the general ODE problem

$$w'(t) = F\big(t, w(t)\big) + G\big(t, w(t)\big), \quad t \geqslant 0, \tag{1.1}$$

☆ Background research for the project LOTOS, which is part of the TASC Project HPCN for Environmental Applications. Hundsdorfer and Verwer acknowledge financial support from the Dutch HPCN program.

* Corresponding author. On leave from University of Kansas, USA. Present address: Delft University of Technology, Faculty of Technical Mathematics and Informatics, P.O. Box 5031, 2600 GA Delft, The Netherlands.

PII S0168-9274(97)00059-7

where F represents the nonstiff part and G represents the stiff part of the system. For the numerical solution of (1.1) we consider *implicit–explicit* (IMEX) linear multistep methods

$$\sum_{j=0}^{k} a_j w_{n+1-j} = \tau \sum_{j=1}^{k} b_j F(t_{n+1-j}, w_{n+1-j}) + \tau \sum_{j=0}^{k} c_j G(t_{n+1-j}, w_{n+1-j}). \tag{1.2}$$

Here $\tau > 0$ denotes the time step and the vectors w_n approximate the exact solution at $t_n = n\tau$. Schemes of this type were introduced by Crouzeix [3] and Varah [9].

A natural way to derive such a method is to start with an implicit method that is known to possess favorable stability properties, and then replace the term $F(t_{n+1}, w_{n+1})$ by a linear combination of explicit terms using extrapolation. If the implicit method has order p and the extrapolation is of order q, the resulting scheme will be of order $\min\{p, q\}$, see [6]. On the other hand, it is not hard to see from the proof of [6] that any consistent IMEX linear multistep method can be decomposed into an implicit scheme and an extrapolation procedure. Direct derivations of the order conditions for IMEX linear multistep methods are given by Ascher et al. [2].

In this paper we will discuss the stability properties of the schemes for the scalar, complex test equation

$$w'(t) = \lambda w(t) + \mu w(t). \tag{1.3}$$

In applications for PDEs, these λ and μ represent the eigenvalues of the nonstiff and stiff part, respectively, found by a Fourier analysis. We will not assume that λ and μ are coupled, so that F and G may contain discretized spatial derivatives in different directions. To simplify the notation, we will make in the following the substitutions $\lambda \to \tau\lambda$ and $\mu \to \tau\mu$. Application of the IMEX scheme then gives

$$\sum_{j=0}^{k} a_j w_{n+1-j} = \lambda \sum_{j=1}^{k} b_j w_{n+1-j} + \mu \sum_{j=0}^{k} c_j w_{n+1-j}. \tag{1.4}$$

As a simple example consider the first order IMEX Euler method

$$w_{n+1} - w_n = \tau F(t_n, w_n) + \tau G(t_{n+1}, w_{n+1}). \tag{1.5}$$

For the linear test equation this gives

$$w_{n+1} = (1 - \mu)^{-1}(1 + \lambda) w_n,$$

and it easily follows that the method is stable whenever λ lies in the stability region of the explicit Euler method, $|1 + \lambda| \leqslant 1$, and μ is in the stability region of the implicit Euler method, $|1 - \mu| \geqslant 1$. As we shall see, this is an exceptional situation. Usually, stability of the individual explicit and implicit methods does not guarantee stability of the combined IMEX method.

In this paper we consider several second order methods, where the implicit method is A-stable. We shall address two questions:

- Suppose that λ lies in the stability region $\mathcal{S}$ of the explicit method. What restrictions are to be placed on the location of μ to have stability?
- What additional restrictions, if any, are to be imposed on the location of λ to ensure that the method is stable for all μ in the left half-plane?

Some examples of IMEX methods that seem interesting for practical applications are given in Section 2. In Section 3 we discuss the restrictions on λ for having stability for arbitrary μ in the left half-plane. In Section 4 we discuss the question of stability of the IMEX methods under the assumption that λ lies in the stability region of the explicit method. Some consequences for CFL restrictions are considered in Section 5, where λ will be an eigenvalue for advection discretizations.

Related stability results for IMEX multistep methods have been derived by Varah [9] and Ascher et al. [2] for the one-dimensional convection–diffusion problem, with central spatial discretizations, where the convection is treated explicitly. For such problems there will be a coupling between the eigenvalues λ and μ. The results presented in this paper are applicable to more general problems and more general spatial discretizations, since λ and μ are considered to be independent of each other and the specific form of the eigenvalues is not prescribed a priori.

Clearly there is a big gap between the test equation (1.3) and the general problem (1.1). Results for (1.3) can be easily extended to linear systems with normal, commuting matrices. Note that if $F = L \otimes I$ and $G = I \otimes M$, with Kronecker product $\otimes$, then F and G will commute. Matrices of this type arise from linear PDE problems with constant coefficients if F and G contain discretized spatial derivatives in different directions. Stability and convergence results for the noncommuting case, but where G is assumed to be negative definite, can be found in Crouzeix [3]. Generalizations for G linear, negative definite and F nonlinear are given in Akrivis et al. [1]. Here we shall restrict ourselves to the scalar, linear case but there is no a priori restriction on the location of the eigenvalues λ and μ other than that they should lie in the stability region of the explicit or implicit multistep method, respectively.

2. Preliminaries

Stability of (1.4) is determined by the location of the roots of the characteristic equation

$$\sum_{i=0}^{k} a_i \zeta^{k-i} - \lambda \sum_{i=1}^{k} b_i \zeta^{k-i} - \mu \sum_{i=0}^{k} c_i \zeta^{k-i} = 0. \tag{2.1}$$

For a root ζ, stability requires that $|\zeta| \leqslant 1$, with strict inequality for multiple roots, see for instance [4,5,7]. If this last condition is omitted, a weak, polynomial instability may occur. The requirement that $|\zeta| \leqslant 1$ is more important, since its violation will lead to an exponential blow-up.

Dividing the equation by ζ^k and making the substitution $z = 1/\zeta$, the characteristic equation reads

$$A(z) - \lambda B(z) - \mu C(z) = 0,$$

where A, B and C are the polynomials

$$A(z) = \sum_{i=0}^{k} a_i z^i, \qquad B(z) = \sum_{i=1}^{k} b_i z^i, \qquad C(z) = \sum_{i=0}^{k} c_i z^i. \tag{2.2}$$

So, for stability we require that all roots satisfy $|z| \geqslant 1$, again with strict inequality if z is a multiple root. A necessary condition for this is

$$A(z) - \lambda B(z) - \mu C(z) \neq 0 \quad \text{for all } |z| < 1. \tag{2.3}$$

Apart from the possibility of multiple roots with modulus 1 this is also a sufficient condition. We shall use (2.3) as a criterion for determining stability. On the boundaries of the stability domains it can then be verified separately whether multiple roots with modulus 1 occur.

In the following we denote by $\mathcal{S}$ the stability region of the explicit method. Its interior int($\mathcal{S}$), where all characteristic roots have modulus less than 1, is given by the *complement* of the set $\{A(z)/B(z)\colon\ |z| \leqslant 1\}$, as can be seen from the above by setting $\mu = 0$. The boundary of the stability region is contained in the root locus curve

$$\{A(e^{i\theta})/B(e^{i\theta})\colon\ \theta \in [-\pi, \pi]\}. \tag{2.4}$$

Below we give some examples of IMEX multistep methods with the stability regions of the explicit methods. The attention will be restricted to second order methods for which the implicit method is A-stable. We shall denote $F_n = F(t_n, w_n)$ and $G_n = G(t_n, w_n)$.

Example 2.1 (Crank–Nicolson leap-frog). Using the explicit midpoint method (leap-frog) for the explicit part with trapezoidal rule (Crank–Nicolson) for the implicit part provides the popular scheme

$$\tfrac{1}{2}(w_{n+1} - w_{n-1}) = \tau F_n + \tfrac{1}{2}\tau(G_{n+1} + G_{n-1}). \tag{2.5}$$

The polynomials (2.2) for this method are

$$A(z) = \tfrac{1}{2}(1 - z^2), \qquad B(z) = z, \qquad C(z) = \tfrac{1}{2}(1 + z^2),$$

and the root locus curve for the stability region of the explicit method is

$$\lambda(\theta) = \frac{1 - e^{i2\theta}}{2e^{i\theta}} = -i \sin\theta, \quad \theta \in [-\pi, \pi].$$

That is, the explicit eigenvalues λ must be restricted to the imaginary axis between $-i$ and i. For the extremal values $\lambda = \pm i$ the roots of the characteristic equation coincide, so we then have a linear instability.

Example 2.2 (Extrapolated BDF). A second order IMEX method can be derived from the two-step backward differentiation formula, with extrapolation $F_{n+1} \approx 2F_n - F_{n-1}$ for the explicit part, thus giving

$$\tfrac{3}{2}w_{n+1} - 2w_n + \tfrac{1}{2}w_{n-1} = \tau(2F_n - F_{n-1}) + \tau G_{n+1}. \tag{2.6}$$

In Verwer et al. [10] this method was applied successfully to a large system (1.1) arising from spatial discretization of an atmospheric transport-chemistry model. The implementation there was slightly different, with $F(2w_n - w_{n-1})$ instead of $2F_n - F_{n-1}$, but for linear stability this is irrelevant.

The polynomials (2.2) are given by

$$A(z) = \tfrac{1}{2}(3 - z)(1 - z), \qquad B(z) = z(2 - z), \qquad C(z) = 1,$$

and the boundary of the explicit stability region $\mathcal{S}$ is parameterized by

$$\lambda(\theta) = \frac{(3 - e^{i\theta})(1 - e^{i\theta})}{2e^{i\theta}(2 - e^{i\theta})}, \quad \theta \in [-\pi, \pi].$$

Example 2.3 (Adams methods). We consider the class of second order Adams type methods, with parameter $c \geqslant 0$,

$$w_{n+1} - w_n = \tfrac{3}{2}\tau F_n - \tfrac{1}{2}\tau F_{n-1} + \tfrac{1}{2}(1+c)\tau G_{n+1} + \tfrac{1}{2}(1-2c)\tau G_n + \tfrac{1}{2}c\tau G_{n-1}. \tag{2.7}$$

Again these methods can be obtained from the implicit formula by extrapolation. The implicit methods are A-stable for any $c \geqslant 0$. For $c = 0$ the implicit method is simply the trapezoidal rule (Crank–Nicolson). The choice $c = \frac{1}{8}$ was considered by Ascher et al. [2]; within this class $c = \frac{1}{8}$ yields maximal damping at $\mu = \infty$. The implicit method with $c = \frac{1}{2}$ was advocated by Nevanlinna and Liniger [8], with regard to maximum norm contractivity.

The polynomials (2.2) are given by

$$A(z) = 1 - z, \qquad B(z) = \tfrac{1}{2}z(3-z), \qquad C(z) = \tfrac{1}{2}(1+c) + \tfrac{1}{2}(1-2c)z + \tfrac{1}{2}cz^2.$$

The boundary of the stability region of the explicit method, the two-step Adams–Bashforth method, is given by

$$\lambda(\theta) = \frac{2(1-\mathrm{e}^{\mathrm{i}\theta})}{\mathrm{e}^{\mathrm{i}\theta}(3-\mathrm{e}^{\mathrm{i}\theta})}, \quad \theta \in [-\pi, \pi].$$

3. Restrictions on explicit eigenvalues for implicit A-stability

Defining $\varphi_\lambda(z) = (A(z) - \lambda B(z))/C(z)$, criterion (2.3) reads

$$\mu \neq \varphi_\lambda(z) \quad \text{for any } |z| < 1. \tag{3.1}$$

We shall apply this criterion to determine under what conditions we have A-stability with respect to the implicit eigenvalue, that is stability for arbitrary $\mu \in \mathbb{C}^-$, the left half-plane. In the first section it was noted already that the IMEX Euler method remains A-stable with respect to the implicit eigenvalues so long as all of the explicit eigenvalues are in the stability region of the explicit method. We can show a similar result for the Crank–Nicolson leap-frog scheme (2.5).

Example 3.1. For scheme (2.5), with $\lambda = -\mathrm{i}\sin\theta$ in the explicit stability region, we have

$$\varphi_\lambda(z) = \frac{1 - z^2 + 2z\mathrm{i}\sin\theta}{1+z^2} = \frac{1 - (z^2 - \bar{z}^2) - |z|^4 + 2\mathrm{i}z\sin\theta(1+\bar{z}^2)}{1 + (z^2+\bar{z}^2) + |z|^4}.$$

The denominator of this last expression is obviously positive for $|z| < 1$. The real part of the numerator is

$$1 - |z|^4 - 2\sin\theta\,\mathrm{Im}\big[z\big(1+\bar{z}^2\big)\big] = \big(1-|z|^2\big)\big[1 + x^2 + y^2 - 2y\sin\theta\big] > 0$$

for any $|z| < 1$, $z = x + \mathrm{i}y$. So A-stability for the implicit eigenvalues μ is preserved as long as the explicit eigenvalues λ are in $\mathcal{S}$.

As we shall see, for the other methods of Examples 2.2 and 2.3 A-stability for the implicit eigenvalues is not preserved for arbitrary $\lambda \in \mathcal{S}$. We define

$$\mathcal{D} = \{\lambda \in \mathbb{C}\text{: (2.1) is stable for any } \mu \in \mathbb{C}^-\}. \tag{3.2}$$

Obviously, $\mathcal{D}$ will be a subset of the closure of the explicit stability domain $\mathcal{S}$. The following lemma gives a characterization for the boundary in terms of the functions $M(\theta) = A(e^{i\theta})/C(e^{i\theta})$ and $N(\theta) = B(e^{i\theta})/C(e^{i\theta})$.

Lemma 3.2. *Suppose* $\operatorname{Re} N(\theta) \not\equiv 0$ *and* $M(\theta)$, $N(\theta)$ *are bounded for all* $\theta \in [-\pi, \pi]$. *Then* $\partial\mathcal{D} \subset \{\lambda(\theta)\text{: } \theta \in [-\pi, \pi]\}$ *with*

$$\lambda(\theta) = \frac{\mathrm{d}}{\mathrm{d}\theta}\left(\frac{M(\theta) + M(-\theta)}{N(-\theta)}\right)\left[\frac{\mathrm{d}}{\mathrm{d}\theta}\left(\frac{N(\theta)}{N(-\theta)}\right)\right]^{-1}. \tag{3.3}$$

Proof. If $\lambda \in \mathcal{D}$ then, according to (3.1), φ_λ maps the interior of the unit disc into the right half-plane. By assumption the image of the unit disc under φ_λ is bounded. For a point on the boundary of $\mathcal{D}$ we thus have

$$\operatorname{Re} \varphi_\lambda(e^{i\theta}) = 0 \tag{3.4}$$

for some point $e^{i\theta}$ on the unit circle. Moreover,

$$\frac{\mathrm{d}}{\mathrm{d}\theta}\operatorname{Re} \varphi_\lambda(e^{i\theta}) = 0, \tag{3.5}$$

which is necessary so that $\operatorname{Re}\varphi_\lambda(e^{i\theta})$ does not become negative for points near $z = e^{i\theta}$ on the unit disk. We can simplify these conditions somewhat, obtaining a single parameterization in terms of the functions M and N, evaluated in the point θ, as follows:

$$\begin{cases} 0 = (\overline{M} - \overline{N}\,\overline{\lambda}) + (M - N\lambda), \\ 0 = (\overline{M}' - \overline{N}'\,\overline{\lambda}) + (M' - N'\lambda). \end{cases}$$

Solving this system for $\lambda = \lambda(\theta)$, we obtain

$$\lambda(\theta) = \frac{-\overline{N}\,\overline{M}' + \overline{N}'\,\overline{M} - \overline{N}M' + \overline{N}'M}{\overline{N}'N - \overline{N}N'} = \frac{\overline{N}(\overline{M}' + M') - \overline{N}'(\overline{M} + M)}{\overline{N}N' - \overline{N}'N},$$

which is equivalent to (3.4). This expression is well defined iff $N(\theta)$ is not identically equal to $\overline{N(\theta)}$. □

For specific methods the boundary of the set $\mathcal{D}$ can be parameterized by evaluating (3.3) for $\theta \in [-\pi, \pi]$. For the IMEX–BDF method (2.6) this leads to a region $\mathcal{D}$ with boundary

$$\lambda(\theta) = -\tfrac{1}{6}(1 - e^{i\theta})(3 - e^{i\theta}), \tag{3.6}$$

see Fig. 1. This region seems only marginally smaller than the explicit stability region $\mathcal{S}$. Note however that near the origin $\mathcal{S}$ stays closer to the imaginary axis than $\mathcal{D}$.

For the IMEX–Adams schemes (2.7) we get the more complicated formula, found by Maple,

$$\lambda(\theta) = P(e^{i\theta})/Q(e^{i\theta}) \tag{3.7}$$

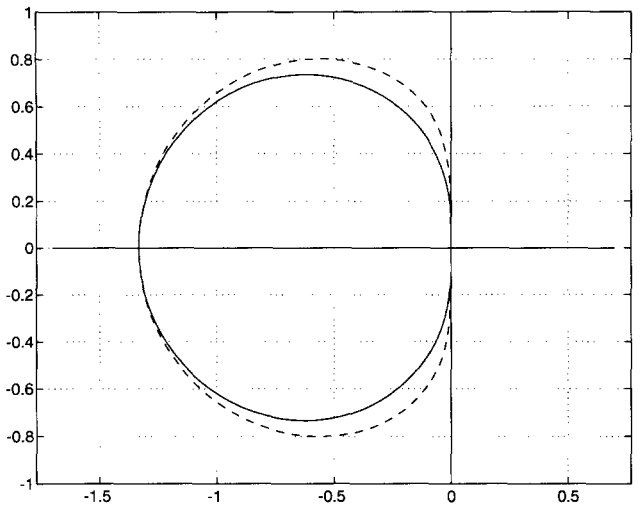

Fig. 1. The explicit stability region $\mathcal{S}$ (dashed) and the region $\mathcal{D}$ for the IMEX–BDF2 method.

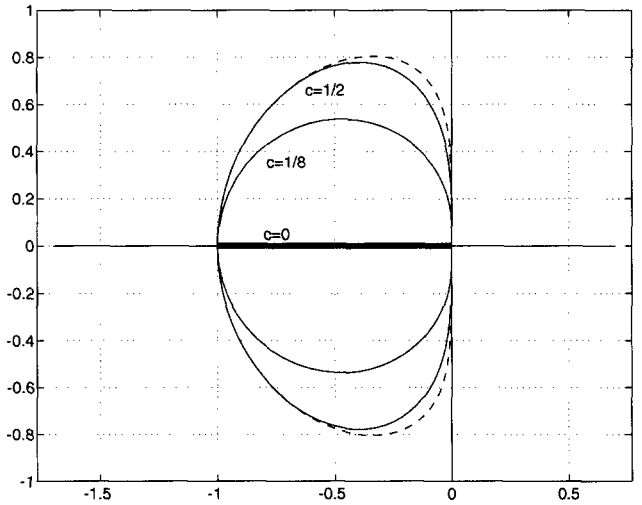

Fig. 2. The explicit stability region $\mathcal{S}$ (dashed) and the regions $\mathcal{D}$ for the IMEX–Adams2 methods with $c = \frac{1}{2}$, $\frac{1}{8}$ and 0.

with

$$
\begin{aligned}
P(z) &= c(z-1)\big(-6cz^3 + 2(5c-6)z^2 - 2(c+12)z^2 - 2(c-2)\big),\\
Q(z) &= 3\big(c+c^2\big)z^4 + 2\big(3-c-4c^2\big)z^3 + 2\big(6+11c+5c^2\big)z^2 + \\
&\quad + 2\big(3-c-4c^2\big)z + 3\big(c+c^2\big).
\end{aligned}
\tag{3.8}
$$

The $\mathcal{D}$ regions for $c = \frac{1}{8}$ and $c = \frac{1}{2}$ are given in Fig. 2. For $c = \frac{1}{2}$ it is close to $\mathcal{S}$, whereas for $c = \frac{1}{8}$ we lose a considerable part of the explicit stability region. For $c = 0$ the lemma does not apply since M and N are not bounded near $\theta = \pi$, and so we consider this method separately.

Example 3.3. For (2.7) with $c = 0$, the Adams–Bashforth Crank–Nicolson method, we have

$$\varphi_\lambda(z) = \frac{2(1-z) - \lambda z(3-z)}{1+z}.$$

This can be written as

$$\varphi_\lambda(z) = 2 - z + (1+\lambda)\chi(z) \quad \text{with } \chi(z) = -\frac{z(3-z)}{1+z}. \tag{3.9}$$

By some calculations it follows that $\operatorname{Re}\chi(e^{i\theta}) = -2 + \cos\theta$. Note that for $\theta \to \pi$ the real part of $\chi(e^{i\theta})$ tends to -3 and its modulus to ∞. Hence χ maps the unit disk into the half plane $\{\zeta \in \mathbb{C}\colon \operatorname{Re}\zeta \geqslant -3\}$ and the imaginary axis lies totally in this image. It follows that the image of the unit disk under φ_λ will have a nonempty intersection with the left half plane if $1 + \lambda$ has a nonzero imaginary part. Therefore λ has to be real to be in $\mathcal{D}$.

Since $\mathcal{D}$ is a subset of $\mathcal{S}$, the only possible values are in the interval $[-1, 0]$. Indeed any λ on this piece of the real negative axis is in $\mathcal{D}$. This can be seen as follows: we have for real λ

$$\operatorname{Re}\varphi_\lambda(e^{i\theta}) = -\lambda(2 - \cos\theta) \geqslant 0 \quad \text{if } \lambda \leqslant 0,$$

and from (3.9) it now follows that the unit disk is mapped into the right half-plane if $\lambda \leqslant 0$ and $1 + \lambda \geqslant 0$.

4. Restrictions on implicit eigenvalues for full explicit stability

Although A-stability is a valuable property, in most practical situations one can settle for less demanding properties, such as $A(\alpha)$-stability. In this section we consider what requirements on μ are needed to ensure stability of the IMEX methods for arbitrary $\lambda \in \mathcal{S}$. The implicit eigenvalues μ are supposed to be in the wedge

$$\mathcal{W}_\alpha = \{\zeta \in \mathbb{C}\colon \, |\arg(-\zeta)| < \alpha\}$$

with angle $\alpha \in (0, \frac{1}{2}\pi)$.

Lemma 4.1. *Suppose that*

$$|\arg(A(z) - \lambda B(z))| \leqslant \tfrac{1}{2}\pi + \beta, \qquad |\arg(C(z))| \leqslant \gamma$$

for all $|z| = 1$ and $\lambda \in \partial\mathcal{S}$, with $\beta + \gamma < \frac{1}{2}\pi$. Then the IMEX scheme will be stable for any $\lambda \in \mathcal{S}$ and $\mu \in \mathcal{W}_\alpha$, with $\alpha = \frac{1}{2}\pi - \beta - \gamma$.

Proof. We have

$$|\arg(\varphi_\lambda(z))| \leqslant |\arg(A(z) - \lambda B(z))| + |\arg(C(z))|.$$

From the assumptions it follows that

$$|\arg(\varphi_\lambda(z))| \leqslant \tfrac{1}{2}\pi + \beta + \gamma$$

for all $|z| \leqslant 1$ and $\lambda \in \mathcal{S}$. Using criterion (3.1), the result follows. □

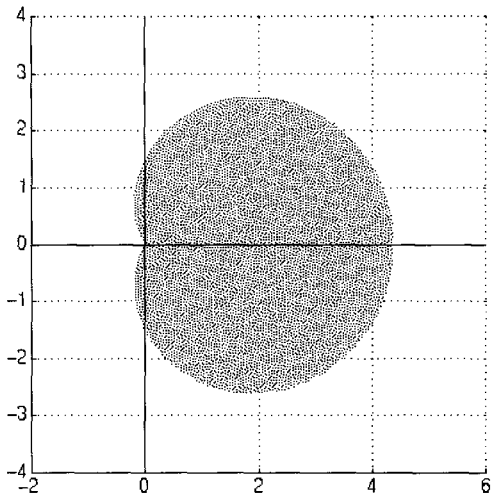

Fig. 3. Exterior of shaded region: stability for μ with arbitrary $\lambda \in \mathcal{S}$ for the IMEX–BDF2 method.

To determine the angle β in the above lemma for the 2-step methods, note that we can write

$$A(z) - \lambda B(z) = A(0)(1 - \rho_1 z)(1 - \rho_2 z),$$

where ρ_1 and ρ_2 are the characteristic roots of the explicit method. For $\lambda \in \partial\mathcal{S}$ we get $|\rho_1| = 1$ and $|\rho_2| \leqslant r$ with some constant $r \leqslant 1$ determined by the explicit method. It follows by geometrical considerations that we can take $\beta = \arcsin r$.

Example 4.2. Consider the IMEX–BDF2 scheme (2.6). The characteristic equation of the explicit method reads

$$\tfrac{3}{2}\zeta^2 - 2(1+\lambda)\zeta + \tfrac{1}{2}(1+2\lambda) = 0,$$

see (2.1) with $\mu = 0$. If $\lambda \in \partial\mathcal{S}$ we can set $\rho_1 = \mathrm{e}^{\mathrm{i}\theta}$ and by some calculations it is seen that

$$\rho_2 = \frac{1}{3}\frac{3\mathrm{e}^{\mathrm{i}\theta} - 2}{2\mathrm{e}^{\mathrm{i}\theta} - 1}, \qquad |\rho_2| \leqslant \tfrac{5}{9}.$$

Further we have $\arg(C(z)) = 0$. Therefore Lemma 4.1 gives stability with angle

$$\alpha = \tfrac{1}{2}\pi - \arcsin\tfrac{5}{9} \approx 0.31\pi. \tag{4.1}$$

The region of those μ for which we have stability with arbitrary $\lambda \in \mathcal{S}$ is given by the *complement* of the set $\{\varphi_\lambda(z)\colon\ \lambda \in \mathcal{S},\ |z| < 1\}$. Although we do not have a parameterization of the boundary of this set, we can make a (crude) picture of it by plotting the value of $\varphi_\lambda(z)$ for sufficiently many $\lambda \in \mathcal{S}$ and $|z| < 1$. In Fig. 3 this region is shown for the IMEX–BDF2 scheme. By zooming in on the origin one can establish an *experimental bound* of the angle α, and for this method it was found that $\alpha \approx 0.32\pi$, which is close to the lower bound (4.1).

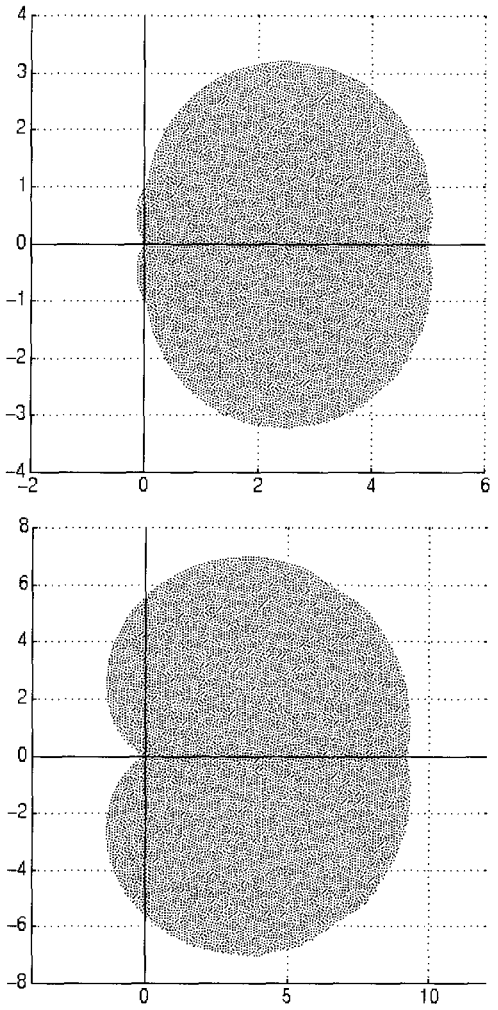

Fig. 4. Exterior of shaded region: stability for μ with arbitrary $\lambda \in \mathcal{S}$ for the IMEX–Adams method with $c = \frac{1}{2}$ (left) and $c = \frac{1}{8}$ (right).

Example 4.3. Consider the IMEX–Adams scheme (2.7). For the 2-step Adams–Bashforth method, with $\lambda \in \partial\mathcal{S}$, we get, similar to the previous example, $\rho_1 = \mathrm{e}^{\mathrm{i}\theta}$ and

$$\rho_2 = \frac{\mathrm{e}^{\mathrm{i}\theta} - 1}{3\mathrm{e}^{\mathrm{i}\theta} - 1}, \qquad |\rho_2| \leqslant \tfrac{1}{2},$$

giving $\beta = \arcsin\frac{1}{2}$.

If $c = \frac{1}{2}$ then $C(z) = \frac{3}{4}(1 + \frac{1}{3}z^2)$, and thus we can take $\gamma = \arcsin\frac{1}{3}$. This gives stability of scheme (2.7) for $\lambda \in \partial\mathcal{S}$ and $\mu \in \mathcal{W}_\alpha$ with

$$\alpha = \tfrac{1}{2}\pi - \arcsin\tfrac{1}{2} - \arcsin\tfrac{1}{3} \approx 0.23\pi. \tag{4.2}$$

As in the previous example we determined from Fig. 4 an experimental bound for α and this was found to be $\approx 0.30\pi$, so here the lower bound (4.2) seems not very close.

If $c = \frac{1}{8}$ then $C(z) = \frac{3}{16}(1 + \frac{1}{3}z)^2$, leading to $\gamma = 2\arcsin\frac{1}{3}$. This gives an angle

$$\alpha = \tfrac{1}{2}\pi - \arcsin\tfrac{1}{2} - 2\arcsin\tfrac{1}{3} \approx 0.12\pi. \tag{4.3}$$

The experimental bound for this method, see Fig. 4, was found to be $\approx 0.14\pi$.

Example 4.4. For the IMEX–Adams scheme (2.7) with $c = 0$ we have $C(z) = \frac{1}{2}(1 + z)$, leading to $\gamma = \frac{1}{2}\pi$. Hence for his case Lemma 4.1 does not provide a positive angle α. Note that Lemma 4.1 only gives a sufficient condition. We show that indeed there is no positive α such that the scheme is stable for all $\lambda \in \mathcal{S}$ and $\mu \in \mathcal{W}_\alpha$.

We have

$$\varphi_\lambda(z) = \frac{2(1-z) - \lambda z(3-z)}{1+z}.$$

Now take $z = -1 + \mathrm{i}\varepsilon + \mathrm{O}(\varepsilon^2)$ on the unit circle and $\lambda = -1 - \mathrm{i}\varepsilon + \mathrm{O}(\varepsilon^2)$ on the boundary of $\mathcal{S}$, see Fig. 2. Then $\varphi_\lambda(z) = -1 + \mathrm{O}(\varepsilon)$, showing that we can have values for $\varphi_\lambda(z)$ arbitrarily close to the negative real axis.

5. CFL restrictions for advection terms

So far we have followed an ODE stability analysis in the sense that the eigenvalues λ and μ were allowed to take on arbitrary complex values in certain bounded or unbounded regions in the complex plane. Of course, in actual applications they are determined by specific spatial operators and selected spatial discretization techniques. Often, the nonstiff part F in Eq. (1.1) emanates from advection and the stiff part G from reaction–diffusion terms. For example, in the study of atmospheric transport-chemistry models, a useful test model is the system $c_t + uc_x + vc_y = \varepsilon c_{zz} + g(t, c)$, where c is a vector of concentrations, $uc_x + vc_y$ models advection in a horizontal wind field, εc_{zz} a vertical turbulent/diffusion process, and $g(t, c)$ stiff chemical reactions, see [10] for instance.

In this section we consider the specific case that λ is associated to the advection term uc_x while μ may still take on arbitrary values. We consider the first and third order upwind biased schemes for discretization on a uniform grid with grid size Δx. Let ν denote the Courant number $|u|\tau/\Delta x$. Then for the first order method we have explicit eigenvalues

$$\lambda = -\nu(1 - \cos\theta + \mathrm{i}\sin\theta), \quad -\pi \leqslant \theta \leqslant \pi, \tag{5.1}$$

whereas in the third order case

$$\lambda = -\tfrac{1}{3}\nu\big((\cos\theta - 1)^2 + \mathrm{i}\sin\theta\,(4 - \cos\theta)\big), \quad -\pi \leqslant \theta \leqslant \pi, \tag{5.2}$$

see for instance [10,11]. Central advection discretization of even order leads to purely imaginary eigenvalues, and among the explicit methods considered here only the leap-frog method (2.5) will be stable.

We consider the restrictions on the Courant numbers ν for all explicit eigenvalues to be in the regions $\mathcal{S}$ or $\mathcal{D}$, introduced in Section 3. The bounds, given in Table 1, have been established experimentally.

For applications, the results for the third order upwind discretizations seem more important than for the first order discretization. It is interesting to note the effect of the apparently moderate restriction for implicit A-stability of the IMEX–BDF2 method on the Courant number. If we demand A-stability

Table 1
CFL restrictions for the IMEX methods (2.6) and (2.7)

	$\mathcal{S}$	$\mathcal{D}$	$\mathcal{S}$	$\mathcal{D}$	$\mathcal{S}$	$\mathcal{D}$
(5.1)	0.66	0.66	0.50	0.50	0.50	0.50
(5.2)	0.46	0.23	0.58	0.16	0.58	0.43
	IMEX–BDF2		Adams, $c = \frac{1}{8}$		Adams, $c = \frac{1}{2}$	

for the stiff eigenvalues, the slightly smaller region $\mathcal{D}$ in Fig. 1 results in a reduction of the maximal Courant number by approximately half. The reason for this is that eigenvalues of the third order upwind scheme are very close to the imaginary axis near zero. In this respect, among the IMEX schemes considered here, the Adams scheme (2.7) with $c = \frac{1}{2}$ gives the best results. However, for practical purposes the results of Section 4 seem more important, and there the largest angle α was obtained for the BDF scheme (2.6).

In conclusion, both the IMEX–BDF method (2.6) and the IMEX–Adams method (2.7) with $c = \frac{1}{2}$ give satisfactory stability results. For third order advection discretization, the Adams scheme allows somewhat larger Courant numbers. On the other hand, the BDF scheme has optimal damping properties for the implicit eigenvalues.

Remark 5.1. The bounds of Table 1 were determined experimentally (using Matlab graphics) and are sufficiently accurate for practical purposes. Upper bounds could be obtained by using the techniques of [11]. For the explicit two-step schemes it is even possible to determine maximal Courant numbers analytically by examining the characteristic polynomial. These examinations are elementary but the derivations involved are lengthy and readily become very cumbersome. In [10] a derivation is given for the explicit scheme in (2.6) and the third order upwind discretization. The final steps in this derivation have been carried out with Maple. To ten decimal digits accuracy, the maximal Courant number computed from this expression equals 0.4617485908.

We have carried out a similar derivation for the explicit Adams scheme (2nd order Adams–Bashforth) and the third order upwind discretization. In this case the maximal CFL number in ten decimal digits accuracy is equal to 0.5801977435. The maximum can be shown to be equal to

$$\min_{0 \leqslant x \leqslant 1} \nu(x),$$

where $\nu(x)$ is the real zero of the cubic equation

$$P_3(x)\,\nu^3 + P_2(x)\,\nu^2 - \tfrac{2}{3} = 0,$$

with

$$P_3(x) = \frac{(Q(x))^2}{162\,(x-1)^2}, \qquad P_2(x) = \tfrac{1}{18}\,Q(x), \qquad Q(x) = (x-1)\big(4x^2 - 5x - 17\big).$$

It can be shown that the above cubic polynomial in ν has only one real root for $|x| \leqslant 1$, which means that $\nu(x)$ is defined by the well known formula of Cardano. However, the minimization over x is very complicated and at this stage Maple has to be used to find the (very long) analytical expression for the maximal Courant number given above.

References

[1] G. Akrivis, M. Crouzeix and C. Makridadis, Implicit–explicit multistep finite element methods for nonlinear parabolic equations, Report 95-22, University of Rennes (1995).
[2] U.M. Ascher, S.J. Ruuth and B. Wetton, Implicit–explicit methods for time-dependent PDE's, *SIAM J. Numer. Anal.* 32 (1995) 797–823.
[3] M. Crouzeix, Une méthode multipas implicite–explicite pour l'approximation des équations d'évolution paraboliques, *Numer. Math.* 35 (1980) 257–276.
[4] E. Hairer, S.P. Nørsett and G. Wanner, *Solving Ordinary Differential Equations* I. *Nonstiff Problems* (Springer, Berlin, 1987).
[5] E. Hairer and G. Wanner, *Solving Ordinary Differential Equations* II. *Stiff and Differential–Algebraic Problems* (Springer, Berlin, 1991).
[6] W. Hundsdorfer and J.G. Verwer, A note on splitting errors for advection–reaction equations, *Appl. Numer. Math.* 18 (1995) 191–199.
[7] J.D. Lambert, *Numerical Methods for Ordinary Differential Systems* (Wiley, Chichester, 1991).
[8] O. Nevanlinna and W. Liniger, Contractive methods for stiff differential equations II, *BIT* 19 (1979) 53–72.
[9] J.M. Varah, Stability restrictions on second order, three-level finite-difference schemes for parabolic equations, *SIAM J. Numer. Anal.* 17 (1980) 300–309.
[10] J.G. Verwer, J.G. Blom and W. Hundsdorfer, An implicit–explicit approach for atmospheric transport-chemistry problems, *Appl. Numer. Math.* 20 (1996) 191–209.
[11] P. Wesseling, Von Neumann stability conditions for the convection–diffusion equation, *IMA J. Numer. Anal.* 16 (1996) 583–598.
[12] Z. Zlatev, *Computer Treatment of Large Air Pollution Models* (Kluwer, Dordrecht, 1995).